Ligand-Promoted Alumina Dissolution in the Preparation of MoO_X/γ-Al_2O_3 Catalysts: Evidence for the Formation and Deposition of an Anderson-type Alumino Heteropolymolybdate

X. Carrier, J. F. Lambert,* and M. Che†

Contribution from the Laboratoire de Réactivité de Surface, URA 1106 CNRS, Université P. et M. Curie, 4 place Jussieu, 75252 Paris Cedex 05, France

Received June 16, 1997[⊗]

Abstract: The deposition of Mo on γ-alumina by the equilibrium adsorption method starting from ammonium heptamolybdate has been studied. Spectroscopic results converge to indicate that a previously unrecognized species, i.e., the Anderson-type heteropolymolybdate $[Al(OH)_6Mo_6O_{18}]^{3-}$, plays a major role in this type of synthesis as it is quantitatively formed in the solution within a few hours, by reaction of the heptamolybdate with dissolved aluminic species. This results in a considerable increase of alumina solubility in conditions generally thought to be nonaggressive. Furthermore, this species is also present in the solid catalyst after deposition, although it is harder to observe than in the liquid phase. A parallel is drawn with a well-known idea from the field of geochemistry, i.e., ligand-promoted oxide dissolution. The relevance of this phenomenon in catalyst preparation is evaluated in realistic conditions corresponding to published studies and/or industrial procedures. It is concluded that strong metal−support interaction in the deposition stage by surface dissolution followed by reaction in the liquid phase is most likely to be an important phenomenon, not only for cationic metal precursors as previously known but also for anionic precursors such as molybdates.

Introduction

The science of heterogeneous catalysts preparation is coming of age. An effort of rationalization is now underway, as witnessed by a series of recent papers that attempt to describe at a fundamental level the phenomena taking place during the successive stages of catalyst synthesis and to draw parallel with other, better understood fields of chemistry (surface science, coordination chemistry, colloid chemistry, geochemistry).[1−5]

One of the issues being raised is that of the role of oxide supports in the inception of metal−support interaction. According to the system under study, the oxide surface may play the role of a simple physical container, a counterion, a supramolecular ligand, or a *bona fide* reagent.[1] The latter case is more frequent than is generally thought: for instance, several reports have described the formation of nickel(II) phyllosilicates (or other M(II) silicates) upon contact of nickel precursors in solution with a silica surface. These Ni-containing phases will of course have properties very different from isolated adsorbed Ni^{II} ions.[6,7]

The formation of such mixed phases may occur by a surface reaction or by support dissolution, followed by recombination with metal ions in the solution and eventually by reprecipitation. The existence of the latter mechanism was nicely demonstrated by Clause et al. for Ni^{II} or Co^{II} deposition on γ-alumina,[8] where hydrotalcite-like mixed phases are formed by dissolution/reprecipitation.

Thus, the importance of support dissolution phenomena may be considered as well-evidenced experimentally, but all existing reports in the field of catalyst preparation are concerned with systems where the metal precursor in solution is a cationic species. This excludes important categories of supported catalysts such as supported molybdates and tungstates. The present study on the MoO_x/Al_2O_3 system was undertaken to fill this gap.

In many studies on supported catalyst preparation, dissolution of the oxide support (Al_2O_3, SiO_2 ...) is neglected because of the low reported solubility product of these oxides.[9,10] Yet, in the already mentioned Ni^{2+},Co^{2+}/γ-Al_2O_3 systems, extensive support dissolution occurred even at "nonaggressive" pH values between 7 and 8.[11−13]

These results can be rationalized by taking into account concepts from the field of *geochemistry*. Geochemists and specialists of soil science have long known that oxide solubility can be profoundly modified by the presence of specific ions in the solution.[14] This modification can have a kinetic or a thermodynamic origin; in fact, it is more easily understandable for anions capable of acting as ligands than for cations.

† Institut Universitaire de France.

[⊗] Abstract published in *Advance ACS Abstracts,* October 1, 1997.

(1) Che, M. In *Proceedings of the 10th International Congress on Catalysis*; Elsevier: Budapest, **1992**; Vol. A, pp 31−68.

(2) Schwarz, J. A.; Contescu, C.; Contescu, A. *Chem. Rev.* **1995**, *95*, 477−510.

(3) Zamaraev, K. I. *Top. Catal.* **1996**, *3*, 1−76.

(4) Lepetit, C.; Che, M. *J. Mol. Catal.* **1996**, *100*, 147−160.

(5) Lambert, J.-F.; Che, M. *Studies in Surface Science and Catalysis*; Elsevier: Amsterdam, 1997; Vol. 109, pp 97−770.

(6) Clause, O.; Kermarec, M.; Bonneviot, L.; Villain, F.; Che, M. *J. Am. Chem. Soc.* **1992**, *114*, 4709−4717.

(7) Kermarec, M.; Carriat, J. Y.; Burattin, P.; Che, M.; Decarreau, A. *J. Phys. Chem.* **1994**, *98*, 12008−12017.

(8) d'Espinose de la Caillerie, J. B.; Kermarec, M.; Clause, O. *J. Am. Chem. Soc.* **1995**, *117*, 11471−11481.

(9) Brunelle, J. P. *Pure Appl. Chem.* **1978**, *50*, 1211−1229.

(10) Baumgarten, E.; Geldsetzer, F. O.; Kirchausen-Düsing, U. *J. Colloid Interface Sci.* **1995**, *173*, 104−111.

(11) The phenomenon of support dissolution is taken into account (for alumina supported catalysts) when the solution containing the metallic precurssor is strongly acidic. This is the case, for example, for the preparation of Pt/γ-Al_2O_3 catalyst from hexachloroplatinate (H_2PtCl_6) solution.[12,13] However, support dissolution is thought to have negligible effects on the final catalyst in this case.

(12) Shah, A. M.; Regalbuto, R. *Langmuir* **1994**, *10*, 500−504.

(13) Santacesaria, E.; Carra, S.; Adami, I. *Ind. Eng. Chem., Prod. Res. Dev.* **1977**, *117*, 11471−11481.

(14) Stumm, W. *Chemistry of The Solid-Water Interface: Process at the Mineral-Water Interface and Particle-Water Interface in Natural Systems*; J. Wiley & Sons: New York, 1992; pp 165−169.

S0002-7863(97)01981-1 CCC: $14.00

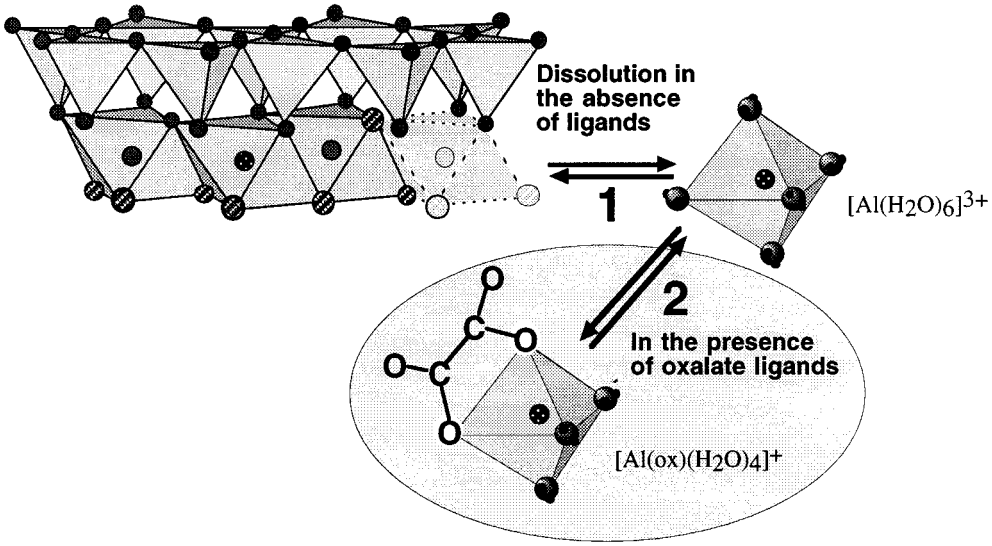

Figure 1. Dissolution of halloysite in (1) the absence of ligands and (2) the presence of oxalate ligands.

Let us consider first the effect of ligands on dissolution kinetics. The specific (presumably innersphere) adsorption of a ligand such as the oxalate ion on an oxide surface can enhance the dissolution rate of this oxide by labilizing the metal−oxygen lattice bonds (Al−O bonds for alumina).[14] Adsorbed oxalate transfers electron density to the surface aluminum ions, thus facilitating the detachment of the surface aluminum from the support lattice. Since the rate-limiting step of mineral dissolution is the detachment of the surface species, it is clear that specific adsorption of a ligand has a kinetic effect on the dissolution of the support.

Support dissolution can also be thermodynamically modified because the formation of ligand−aluminum complexes in solution will enhance the solubility of aluminum oxides by consuming the aluminum ions in solution. The dissolution reaction is then shifted to the right. Thus, the total aluminum concentration in solution is drastically modified in the presence of ligands with an affinity for aluminum ions. This effect has been evidenced, for example, in the oxalate/halloysite system (halloysite is an aluminosilicate clay mineral)[15] (Figure 1).

These concepts may easily be transferred to systems such as MoO_x/Al_2O_3, which is the subject of the present study. The only difference is that we have to consider inorganic ligands instead of the organic ligands (as oxalate) more common in geochemistry.

The Mo precursor most commonly used for MoO_x/Al_2O_3 synthesis is ammonium heptamolybdate. The Al^{III}-complexing ability of the heptamolybdate ion has been the subject of some studies in homogeneous solutions.[16,17] In fact, in the presence of Al^{III} ions, the isopolymolybdate can yield the Anderson-type heteropolymolybdate with formula $[Al(OH)_6Mo_6O_{18}]^{3-}$, hereafter referred to as $[AlMo_6]$.

We can thus expect a thermodynamic effect of molybdates on the solubility of alumina. Öhmann[18] has indeed calculated such an effect on the solubility of gibbsite (aluminum hydroxide, $Al(OH)_3$) which increases by 2 orders of magnitude at pH 5 in the presence of molybdates.

The structure of $[AlMo_6]$, illustrated in a later section of this paper, is planar and built by seven edge-sharing octahedra. The approximate symmetry is D_{3d}, different from that of the heptamolybdate $[Mo_7O_{24}]^{6-}$. The aluminum lies in the central octahedron, surrounded by six OH.[17] The six OH protons are nonacidic; they are essential for stabilizing the compound. Indeed, the deprotonated species is not reported in the litterature with Al^{3+} as the central atom, be it in the liquid or in the solid state.[16−18]

The present work shows that the Anderson-type heteropolymolybdate $[AlMo_6]$, which was not previously taken into account in the study of MoO_x/Al_2O_3 catalysts, is in fact of major importance in this system: in some synthesis conditions, it can be the only molybdenum-containing species deposited on the alumina support. We first establish the formation of $[AlMo_6]$ in molybdate solutions in contact with alumina through a comparative spectroscopic study of these solutions and the reference heteropolymolybdate; we then show that $[AlMo_6]$ is present in the adsorbed phase and conclude with a discussion of the generality of these findings.

Experimental Section

Samples Preparation. The support was a γ-alumina from Rhône-Poulenc, with surface area = 189 $m^2\ g^{-1}$ and a pore volume of 0.64 $cm^3\ g^{-1}$. Prior to use, the alumina pellets were ground in a mortar and the fraction $150 < \phi < 400$ μm was collected by sieving.

The catalysts were prepared by the equilibrium adsorption method. Ground alumina was suspended in distilled water with an oxide/water ratio of 1 g/100 mL. Ammonium heptamolybdate ($(NH_4)_6Mo_7O_{24}\cdot 4H_2O$, Merck) was added up to the concentration [Mo] = 6.4×10^{-2} M. The suspensions were stirred at room temperature for variable times (1 h to 1 month). The pH was kept constant throughout equilibration by addition of either concentrated HNO_3 or NH_3. After filtration, the solid phases were washed three times with distilled water and left to dry under air at room temperature. The filtrates were kept for analysis.

Elemental analyses of both solid phases and filtrates were performed by the Laboratoire d'Analyses Elementaires (CNRS, Vernaison, France) by inductively coupled plasma/atomic emission spectroscopy (ICP/AES). Relative errors are in the ±2% range. All of the elemental analysis results are reported with respect to solids dried at 80 °C for 18 h, in order to avoid any differences due to the hydration state of the catalysts.

The reference heteropolyanion salt $K_3[Al(OH)_6Mo_6O_{18}]$ was synthesized along procedures published in the literature, and its nature was ascertained by X-ray diffractometry[19] (see the Supporting Information).

(15) Smith, R. W. *Coord. Chem. Rev.* **1996**, *149*, 86−88.
(16) Tsigdinos, G. A. *Top. Curr. Chem.* **1978**, *76*, 38−41.
(17) Pope, M. T. *Heteropoly and Isopoly Oxometalates*; Springer-Verlag: Berlin, 1983; pp 21−23, 81−82.
(18) Öhman, L. O. *Inorg. Chem.* **1989**, *28*, 3629−3632.
(19) Lee, H. Y.; Park, K. M.; Lee, U.; Ichida, H. *Acta Crystallogr.* **1991**, *C47*, 1959−1961.

NMR Spectroscopy. Liquid-state NMR spectra were obtained at 9.4 T over a Bruker MSL 400 spectrometer. Simple one-pulse sequences with phase cycling were used. For ^{27}Al, the Larmor frequency was 104.26 MHz the pulse length was 1 μs, and the recycle delay was 500 ms. A 0.1 M solution of aluminum nitrate was used as the 0 ppm reference. For ^{95}Mo, the Larmor frequency was 26.08 MHz, the pulse length was 5 μs, and the recycle delay was 1 s. A 2 M solution of sodium molybdate was used as the 0 ppm reference. The solid-state ^{27}Al NMR experiments were carried out at 11.7 T over a Bruker ASX 500 spectrometer fitted with a high-speed magic angle spinning (MAS) probe. The Larmor frequency was 130.32 MHz. We used both single-pulse MAS and proton cross-polarization (CP) MAS. For single-pulse MAS experiments, the pulse length was 5 μs, the recycle delay was 1 s, and the MAS rate was $\omega_{rot} = 11$ kHz. For cross-polarization experiments, the contact time was 1 ms and the MAS spinning rate was $\omega_{rot} = 8$ kHz.

Infrared Spectroscopy. Samples were dispersed in anhydrous KBr pellets, and their spectra were recorded on a Bruker IFS 66V spectrometer equipped with a DTGS detector, with a resolution of 4 cm^{-1}. For supported catalysts, the broad and intense absorption bands arising from the support were minimized through subtraction of the IR spectrum of the bare alumina.

Raman Spectroscopy. The spectra were recorded on a Jobin-Yvon U1000 spectrometer with a double monochromator equipped with an AsGa photomultiplier and photon counting detection. For liquid-state measurements, the excitation source was the 514.5 nm line of an Ar^+ laser (Coherent) and the laser power was adjusted to 200 mW. The resolution was set to 4 cm^{-1}. We used 300 μL quartz cells for sampling.

For solid-state measurements, we used the 488 nm line of the Ar^+ laser with the power adjusted to 80 mW. The resolution was set to 2 cm^{-1}. In order to avoid decomposition by the laser beam, samples were mounted on a disc rotated at about 1000 Hz. This disc was mounted at a 45° angle from the incident beam; in order to remove parasite lines from the Ar^+ plasma, an interferential filter was placed before the sample. Raman measurements were carried out on air-dried samples.

Thermogravimetric Analysis (TGA). The thermograms were recorded on a Seiko SSC 5200H thermal analyzer. The samples were placed in a platinum crucible and heated either at 10 °C min^{-1} under a 100 mL min^{-1} nitrogen flow or at 3 °C min^{-1} under a 200 mL min^{-1} oxygen flow. The reference was an empty platinum crucible.

Computation of Equilibrium Concentrations. We used the TOT software[20] for computing alumina solubility curves. This software calculates the concentration of aqueous species in equilibrium from their equilibrium constants of formation. We computed all of the equilibria with a theoretical ionic strength of 0 (i.e, activity = concentration).

Results

Characterization of the Reference Heteropolyanion $K_3[Al(OH)_6Mo_6O_{18}]$: Thermal Analysis and Elemental Analyses. In thermogravimetric analysis, the derivative of the weight loss thermogram (DTG) of the reference compound gives four maxima at 62, 100, 130, and 245 °C (10 °C min^{-1}, N_2 flow). Changing to other conditions with a slower temperature ramp (3 °C min^{-1}, O_2 flow) shifts the peak maxima to lower temperatures (47, 84, 104, and 227 °C, respectively) but does not affect the quantification significantly. The first three peaks can be attributed to the loss of hydration water: approximatively four water molecules per polyanion are lost in the first step, 1.5 in the second, and 1.5 in the third, giving a total of seven hydration water molecules.

The weight loss respectively observed at 245 or 227 °C corresponds to three water molecules per polyanion and is attributed to the condensation of the six hydroxyls around the central aluminum. Thus, the Anderson-type heteropolyanion is destroyed between 230 and 250 °C, in good agreement with the data reported by Tsigdinos[16] for the chromium-containing isomorphous compound $K_3[Cr(OH)_6Mo_6O_{18}]\cdot 7H_2O$.

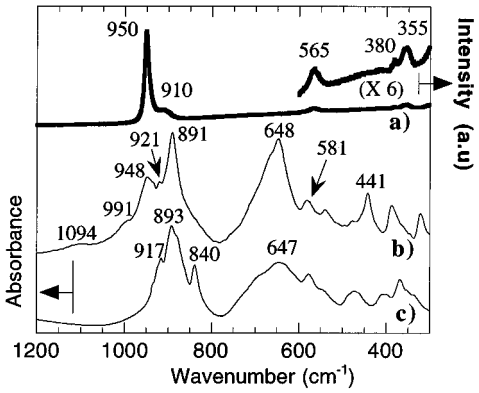

Figure 2. (a) Raman spectrum of $Al(OH)_6Mo_6O_{18}^{3-}$ *in liquid state*; (b) IR spectrum of $K_3[Al(OH)_6Mo_6O_{18}]$ *in solid state*, and (c) IR spectrum of $(NH_4)_6Mo_7O_{24}$ *in solid state* in the 1200−200 cm^{-1} region.

We can thus write the chemical formula for our reference compound as $K_3[Al(OH)_6Mo_6O_{18}]\cdot 7H_2O$. The former formula is in good agreement with the elemental analysis results: 45.0 wt % Mo (theoretical, 46.6 wt %) and 2.2 wt % Al (theoretical, 2.2 wt %).

Molecular Characterization of the Reference Heteropolyanion $Al(OH)_6Mo_6O_{18}^{3-}$: Spectroscopic Data. IR and Raman Spectroscopies. Figure 2 compares the Raman spectrum of $[AlMo_6]$ *in the liquid state* and the IR spectra of $K_3[Al(OH)_6Mo_6O_{18}]$ and $(NH_4)_6Mo_7O_{24}$ *in the solid state*.

In the Raman spectrum of $[AlMo_6]$, five distinct bands are observed (spectrum a). The very intense band at 950 cm^{-1} (with a shoulder at 910 cm^{-1}) can be attributed to Mo═O stretch;[21] the band at 565 cm^{-1} is due to symmetric Mo−O−Mo stretches and two bands at 380 and 355 cm^{-1} are due to Mo═O bending modes. Goncharova et al.[22] reported a band at 212 cm^{-1} which can be attributed to Mo−O−Mo deformation (this band is probably hidden by the Rayleigh line in our case).

We can clearly distinguish this spectrum from that of the heptamolybdate[21] (not presented here), although the most intense band for $(NH_4)_6Mo_7O_{24}$ is located at 943 cm^{-1}, which is very close to the one found at 950 cm^{-1} for $[AlMo_6]$. The heptamolybdate, in addition to showing little intensity at 565 cm^{-1} (five times smaller than the peak at 320−360 cm^{-1}), has a band located at 898 cm^{-1} instead of at 910 cm^{-1} for the Anderson-type species. As for the monomolybdate (MoO_4^{2-}), it is characterized by three bands[21] at 898, 842, and 320 cm^{-1}. Thus, we may consider Raman bands at 565 and 910 cm^{-1} as diagnostic of the presence of the Anderson-type heteropolyanion $[AlMo_6]$.

Regarding the IR spectra, the most intense bands of the Anderson-type heteropolyanion in the 1200−200 cm^{-1} region (spectrum b) are due to to Mo═O streches and Mo−O−Mo symmetric stretches[21] and are located at 948 and 891 cm^{-1} for $\nu_{Mo=O}$ and 648 cm^{-1} for $\nu_{Mo-O-Mo}$ in good agreement with literature data.[23,24] The latter is not diagnostic for the heteropolyanion since the heptamolybdate has bands with very close maxima in this region. The two weak bands located at 1094 and 991 cm^{-1} look more interesting in this respect. In

(20) Rosset, R.; Bauer, D.; Desbarres, J. *TOT Version 2.00*; Ecole Supérieure de Physique et de Chimie Industrielles de la Ville de Paris: Paris, 1987.

(21) Griffith, W. P.; Lesniak, P. J. B. *J. Chem. Soc. A* **1969**, *7*, 1066−1071.

(22) Goncharova, O. I.; Boreskov, G. K.; Yurieva, T. M.; Yurchenko, E. N.; Boldyera, N. N. *React. Kinet. Catal. Lett.* **1981**, *16*, 349−353.

(23) Fuchs, J.; Brüdgam, I. *Z. Naturforsch.* **1977**, *32b*, 403−407.

(24) Goncharova, O. I.; Davydov, A. A.; Yur'eva, T. M. *Kinet. Catal.* **1984,** *25*, 124−129.

aluminum hydroxides,[25] which contain $Al(OH)_6$ octahedra, and in metallic hydroxo salts of the $M(OH)_6$ type[26] (e.g., $K_2Pt(OH)_6$), bands between 900 and 1200 cm^{-1} have been assigned to OH bending vibrations (δ_{OH}). Furthermore, Fuchs and Brüdgam[23] studied a series of protonated Anderson-type heteropolymolybdates of general formula $[M(OH)_6Mo_6O_{18}]^{x-}$ ($M = Fe^{3+}$, Al^{3+}, Ni^{2+}, Cu^{2+} ...). All of these compounds exhibit a strong IR band between 930 and 945 cm^{-1} and a weaker one above 1000 cm^{-1}. In contrast, the molybdotellurate $[TeMo_6O_{24}]^{6-}$, which is known not to be protonated, exhibits a strong IR band at 933 cm^{-1} but does not show any band above 1000 cm^{-1}. Thus, Fuchs and Brüdgam proposed to assign the weak band above 1000 cm^{-1} to OH groups vibrations. The position reported for $Al(OH)_6Mo_6O_{18}^{3-}$ was 1008 cm^{-1} (instead of 991 cm^{-1} in our case), but one must notice that the samples studied by Fuchs and Brüdgam had been crystallized from nonaqueous organic media: therefore, the pattern of H-bonding of the OH groups may be different.

In view of these data, we assign the band located at 1094 cm^{-1} to a bending vibration arising from the OH of the central octahedra; we propose also to assign the band located at 991 cm^{-1} to an OH bending vibration, although with less confidence.

The infrared spectrum of ammonium heptamolybdate (spectrum c) has already been reported.[21] This spectrum is not very different from that of the Anderson-type polyanion as regards to the Mo═O and Mo−O−Mo vibrations, except for the sharp band at 840 cm^{-1} and the absence of Mo−O vibrations above 920 cm^{-1}.

^{95}Mo Liquid-State NMR. The ^{95}Mo liquid-state NMR spectrum of the Anderson-type polyanion shows a broad peak at −20 ppm (line width = 520 Hz; Figure 3A, spectrum b). Gheller et al.[27] reported a peak at −18 ppm with a line width of only 290 Hz (^{95}Mo Larmor frequency = 13.0 Mhz). The difference in line width can arise from the fact that they recorded their spectrum at 50 °C instead of room temperature, which should lead to a more efficient motional averaging. Ammonium heptamolybdate gives one peak at +33 ppm with a line width of 220 Hz (Figure 3A, spectrum a) in good agreement with the results of Luthra and Cheng[28] (+35 ppm, line width = 185 Hz, for a ^{95}Mo Larmor frequency = 26.1 MHz). The monomolybdate ion was chosen as the 0 ppm reference because it gives a very sharp peak.

^{27}Al Liquid-State NMR. The ^{27}Al liquid-state NMR of the Anderson-type polyanion reveals a single peak at +15.5 ppm (line width = 50 Hz, spectrum a, Figure 3B, in agreement with the results of Akitt and Farthing[29] and Öhmann.[18] No other aluminic species likely to be found in our systems resonates near this frequency. Thus, it appears that both ^{95}Mo and ^{27}Al liquid-state NMR can give unambiguous identification of the heteropolymolybdate. However, ^{27}Al NMR is faster and easier to implement.

^{27}Al Solid-State MAS NMR. We have also performed solid-state ^{27}Al MAS NMR on our reference compound. Its spectrum is shown in Figure 3B (spectrum b) and shows one peak at δ = 13.2 ppm. This peak is relatively narrow (line width = 420 Hz), in keeping with the quasi-octahedral local symmetry of the Al site. The value of δ is close to that found in the liquid state. The small variation is probably due to a difference in quadrupolar effects at the higher field used for solid-state NMR.

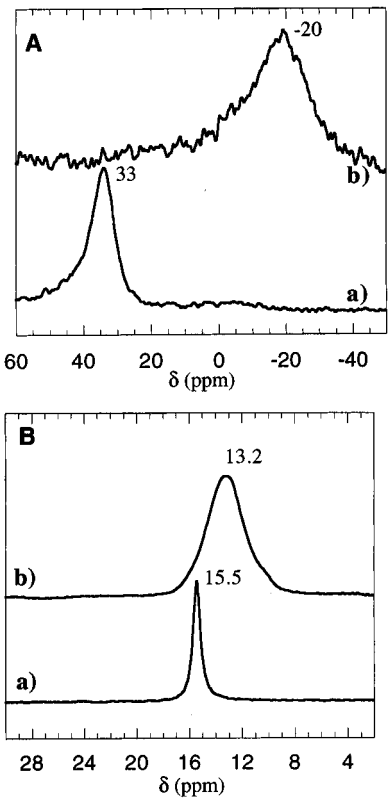

Figure 3. NMR characterization of $[AlMo_6]$. (A) ^{95}Mo liquid-state NMR spectra of (a) $Mo_7O_{24}^{6-}$ ([Mo] = 1 M, pH 5.5) and (b) $Al(OH)_6Mo_6O_{18}^{3-}$ ([Al] = 0.1 M, pH 4). (B) ^{27}Al NMR spectra of (a) $Al(OH)_6Mo_6O_{18}^{3-}$ in liquid state and (b) $K_3[Al(OH)_6Mo_6O_{18}]$ in solid state (MAS NMR).

UV−Vis Spectroscopy. UV−vis spectra of both $K_3[Al(OH)_6Mo_6O_{18}]$ and $(NH_4)_6Mo_7O_{24}$ in the solid state (see the Supporting Information) both exhibit four absorption bands (O^{2-} to Mo^{6+} charge transfers) at 200, 220−230, 260−290 and 310−330 nm. In good agreement with these results, Fournier et al.[30] reported bands at 225, 275−280, and 300−305 nm for ammonium heptamolybdate. It is thus obvious that the two species cannot be discriminated on the basis of UV−vis spectroscopy; this arises from the fact that both compounds are built from edge-sharing molybdenum octahedra.

For easier reference, we have gathered the characteristic spectroscopic features of $[AlMo_6]$ in Table 1.

Identification of the Mo-containing Species in the Liquid Phases after Adsorption of Ammonium Heptamolybdate on γ-Al_2O_3. ^{27}Al Liquid-State NMR. The ^{27}Al NMR spectra of the filtrates obtained after each adsorption experiment are given in Figure 4. All of the spectra have been normalized for the number of scans in order to allow quantitative comparison.

The appearance of the spectra depends on the equilibration pH. For all pH values ≤ 6.5, after an equilibrium time of 7 days, all filtrates show a single peak at 15.5 ± 0.2 ppm (Figure 4A). The integrated intensity of the peak at 15.5 ppm in different filtrates are in agreement with the aluminum contents found by elemental analysis (see the Supporting Information), indicating that no NMR-silent Al-containing species are present (this was not a foregone conclusion since, e.g., octahedral Al

(25) Vivien, D.; Stegmann, M. C.; Mazière, C. *J. Chim. Phys.* **1973**, *70*, 1502−1508.
(26) Maltese, M.; Orville-Thomas, W. J. *J. Inorg. Nucl. Chem.* **1967**, *29*, 2533−2544.
(27) Gheller, S. F.; Sidney, M.; Masters, A. F.; Brownlee, R. T. C.; O'Connor, J. M.; Wedd, A. G. *Aust. J. Chem.* **1984**, *37*, 1825−1832.
(28) Luthra, N. P.; Cheng, W.-C. *J. Catal.* **1987**, *107*, 154−160.
(29) Akitt, J. W.; Farthing, A. *J. Chem. Soc., Dalton Trans.* **1981**, 1615−1616.
(30) Fournier, M.; Louis, C.; Che, M.; Chaquin, P.; Masure, D. *J. Catal.* **1989**, *119*, 400−414.
(31) Akitt, J. W.; Farthing, A. *J. Magn. Reson.* **1978**, *32*, 345−352.
(32) Chen, Q.; Zeng, W.; Chen, X.; Gu, S.; Yang, G.; Zhou, H.; Yin, Z. *Thermochim. Acta* **1995**, *253*, 33−39.

Table 1. Characteristic Spectroscopic Features of [AlMo$_6$] as Compared to Those of Mo$_7$O$_{24}^{6-}$ (Diagnostic Features for [AlMo$_6$] in Bold)

	[AlMo$_6$] (K$^+$ salt in solid state)	Mo$_7$O$_{24}^{6-}$ (NH$_4^+$ salt in solid state)
liquid-state Raman (cm^{-1})	950, **910**, **565**, 380, 355	943, 898, 362, 320 ref 21
solid-state IR (cm^{-1})	**1094**, **991**, **948**, 891, 648	917, 893, 840, 647
^{95}Mo liquid-state NMR	**−20** ppm	33 ppm (main peak)
^{27}Al liquid-state NMR	**15.5** ppm	
^{27}Al solid-state NMR	**13.2** ppm	
UV−vis solid state (nm)	200, 220−230, 260−290, 310−330	200, 220−230, 260−290, 310−330

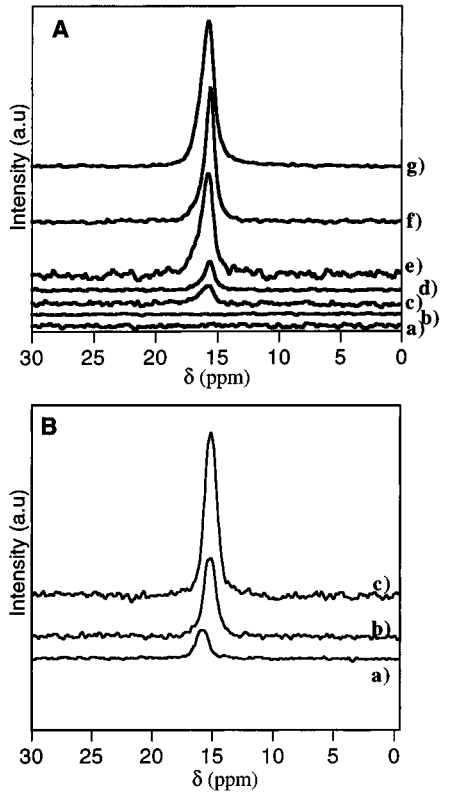

Figure 4. ^{27}Al liquid-state NMR spectra of filtrates obtained after equilibrium adsorption. (A) Equilibrium time of 168 h at varying pH values: (a) pH 8, (b) pH 7, (c) pH 6.5, (d) pH 6.3, (e) pH 6.1, (f) pH 5.1, (g) pH 4. (B) Equilibration pH 4, with varying equilibrium times: (a) 1 h, (b) 7 h, (c) 24 h.

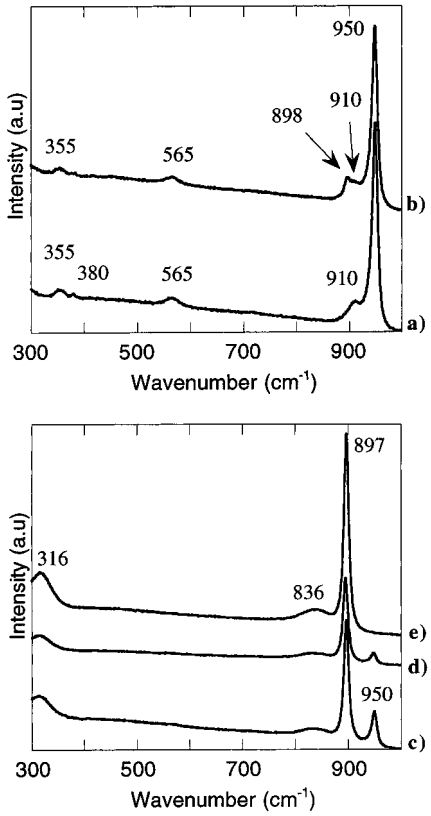

Figure 5. Raman spectra in aqueous solution of filtrates obtained after 168 h of equilibrium at (a) pH 4, (b) pH 5.1, (c) pH 6.3, (d) pH 6.5, and (e) pH 7.

in the Keggin ion [Al$_{13}$] would be undetectable under these conditions[31]).

The data for the short equilibration times (≤24 h, Figure 4B) indicate that the peak at 15.5 ppm can be seen even after 1 h of equilibration at pH 4 (spectrum a). The intensity of this peak increases with time (cf., spectra b and c, at 7 and 24 h). It is also present at pH 6.1 after 24 h of equilibrium (not shown).

It can be concluded that [AlMo$_6$] is spontaneously formed within less than 1 h when ammmonium heptamolybdate solutions are contacted with alumina at pH 4, and within less than 24 h at pH ≤ 6.5.

Raman Spectroscopy. ^{27}Al NMR gives information about the presence of the [AlMo$_6$] heteropolyanion in the solution but does not indicate if isopolymolybdates are still present. Therefore, the Raman spectra of the filtrates obtained after 7 days of equilibration were recorded and are shown in Figure 5.

The spectrum of the solution equilibrated at pH 4 for 168 h (spectrum a, Figure 5) is identical to that of the reference compound [AlMo$_6$] (cf., spectrum a, Figure 2). In particular, the features characteristic of the heptamolybdate and monomolybdate ions are not observed. Therefore, the only detectable molybdate species in solution is the alumino polymolybdate.

At pH 5 (spectrum b, Figure 5), the band at 565 cm^{-1} and the shoulder at 910 cm^{-1} typical of the Anderson-type species are still present but a new shoulder appears at 898 cm^{-1}, which can be assigned to the heptamolybdate species. The conclusion is that both [AlMo$_6$] and [Mo$_7$O$_{24}$]$^{6-}$ are present in the solution, with the latter a minority species.

In the solutions with pH 6.3 and 6.5 (spectra c and d), three bands at 897, 836, and 316 cm^{-1} can be assigned to MoO$_4^{2-}$ while one band at 950 cm^{-1} of lower intensity than that at 897 cm^{-1} may be due either to [AlMo$_6$] or to [Mo$_7$O$_{24}$]$^{6-}$. We know from ^{27}Al NMR that some [AlMo$_6$] species are indeed present.

At pH 7 (spectrum e), the only species that can be evidenced by Raman spectroscopy is MoO$_4^{2-}$ (bands at 897, 836, and 316 cm^{-1}).

Liquid-State ^{95}Mo NMR. An attempt was made to record the ^{95}Mo NMR spectra of the solutions obtained after 7 days of equilibration, to confirm Raman data. However, even with the relatively high Mo concentration used ([Mo] = 6.4 × 10^{-2} M), the obtention of good-quality spectra needed a long-time accumulation (more than 9 h). Despite the low signal to noise ratio, we could resolve one broad peak at −20 ppm in the

(33) Castet, S.; Dandurand, J. L.; Scott, J.; Gout, R. *Geochim. Cosmochim. Acta* **1993**, *57*, 4869−4884.

(34) *CRC Handbook of Chemistry and Physics*, 61st ed.; CRC Press, Inc.: Boca Raton, FL, 1980; pp D71, D74.

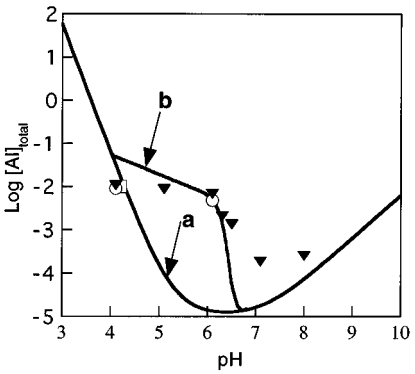

Figure 6. Aluminum content in the liquid phase as a function of pH for different equilibrium times ([Al] in mol L^{-1}): 24 h (circles), 168 h (triangles), 672 h (squares). Theoretical solubility curves of γ-Al_2O_3 calculated (a) from data shown in Table 2 and (b) in the presence of a molybdate solution (6.4×10^{-2} M) from data of ref 18.

Table 2. Thermodynamic Data for Aluminum Aqueous Species and for γ-Alumina

species	ΔG_f°, 298 K (kJ mol^{-1})	refs
γ-Al_2O_3	−1564.2	32
Al^{3+}	−487.7	33
$Al(OH)^{2+}$	−696.3	33
$Al(OH)_2^+$	−903.7	33
$Al(OH)_3$	−1109.2	33
$Al(OH)_4^-$	−1305.4	33
H_2O	−237.2	34
OH^-	−157.3	34

solution at pH 4 (168 h), which is assignable to [$AlMo_6$]. There was no other peak which could be attributed to other type of molybdate species. Thus, in the only case where it was attempted, ^{95}Mo NMR confirmed the conclusions of Raman spectroscopy.

Dissolution of γ-Al_2O_3. We have plotted the aluminum contents of the liquid phases as a function of pH and for different equilibration times in Figure 6. First of all, where kinetic data are available, it is obvious that the aluminum solubility does not increase much with equilibrium time after 24 h. The equilibrium for alumina dissolution is reached at worse in a matter of hours in our systems.

Figure 6 also compares experimental data with theoretical predictions taking into account the various relevant chemical equilibria.

Our computations were based on equilibrium constants derived from published thermodynamic data, as shown in Table 2.

First, we considered the following reactions which do not involve molybdic species:

$$2Al^{3+} + 6OH^- \rightleftharpoons Al_2O_3 + 3H_2O \quad \log K_S{}^1 = 62.47 \quad (1)$$

$$Al^{3+} + OH^- \rightleftharpoons Al(OH)^{2+} \quad \log K_S{}^2 = 8.95 \quad (2)$$

$$Al^{3+} + 2OH^- \rightleftharpoons Al(OH)_2{}^+ \quad \log K_S{}^3 = 17.76 \quad (3)$$

$$Al^{3+} + 3\,OH^- \rightleftharpoons Al(OH)_3 \quad \log K_S{}^4 = 26.21 \quad (4)$$

$$Al^{3+} + 4\,OH^- \rightleftharpoons Al(OH)_4{}^- \quad \log K_S{}^5 = 33.03 \quad (5)$$

The total aluminum content in the solution in equilibrium with alumina was then $[Al]_{total} = [Al^{3+}] + [Al(OH)^{2+}] + [Al(OH)_2{}^+] + [Al(OH)_3] + [Al(OH)_4{}^-]$.

This approach, neglecting polymeric species (such as the "-[Al_{13}]" Keggin complex and the trimeric species $Al_3(OH)_4{}^{5+}$), is generally used in the literature and considered to be self-consistent since, at the low [Al_t] concentrations that result, such polymeric species are unlikely to form to large extents.[35]

Table 3. Mo Contents of Solid Phases after Equilibration in Various Conditions

pH	equilibrium time (h)	Mo loading (wt %)[a]
4	1	4.6
	7	5.2
	24	5.5
	168	5.8
	672	8.8
5.1	168	5.4
6.1	24	4.4
	168	5.1
6.3	168	5.3
6.5	168	4.7
7	168	3.0
8	168	1.5

[a] Mo loading of the catalyst after three washing steps and drying at 80 °C during 18 h.

As shown in Figure 6 (curve a), very low $[Al]_t$ concentrations are predicted in the pH range of our study, in contradiction with experiment. This is not surprising since "$[Al^{3+}]$", which is in fact shorthand for $[Al(H_2O)_6]^{3+}$, reacts with molybdate in solution by

$$6H^+ + Al^{3+} + 6MoO_4{}^{2-} \rightleftharpoons [Al(OH)_6Mo_6O_{18}]^{3-} \quad (6)$$

shifting eq 1 to the left. Alumina solubility is therefore drastically modified in the presence of molybdates, accounting for the results reported in figure 6. The solubility curve labeled b in Figure 6 has been calculated by taking into account data published by Öhman[18] for eq 6 ($\log K^6 = 50.95$) and for polymerization/depolymerization reactions of isopolymolybdates (see Table I in ref 18) such as

$$8H^+ + 7MoO_4{}^{2-} \rightleftharpoons Mo_7O_{24}{}^{6-} + 4H_2O \quad (7)$$

In the quoted study, Öhman in fact considered an effect similar to ours for the dissolution of aluminum hydroxide

$$Al(OH)_3 + 3H^+ \rightleftharpoons Al^{3+} + 3H_2O \quad (8)$$

and predicted a strong increase in the solubility of $Al(OH)_3$ as a consequence of [$AlMo_6$] formation, especially between pH 5 and 6.

The agreement between the theoretical curve and the experimental points is not perfect at basic pH values, but qualitatively speaking, there is no doubt that the presence of molybdates in solution drastically increases the solubility of γ-alumina.

Characterization of the Solid Phases after Equilibrium Adsorption: (i) Amount of Mo Deposited. The amounts of Mo deposited after equilibration in various conditions are an important parameter in the following discussion and are therefore summarized in Table 3.

(ii) Solid-State ^{27}Al NMR. The results of the preceding paragraphs concerned the identification of the [$AlMo_6$] anion in solution. Our next goal was to determine if this species was also present in the solid phase after adsorption. In principle, this is a more difficult task, since we have to discriminate the weak signal arising from the central aluminum of a limited number of [$AlMo_6$] species adsorbed on the surface of γ-Al_2O_3 from the strong signal of the aluminum atoms of the unmodified

(35) Baes, C. F.; Mesmer, R. E. *The Hydrolysis of Cations*; Wiley: New York, 1976; pp 112−123.

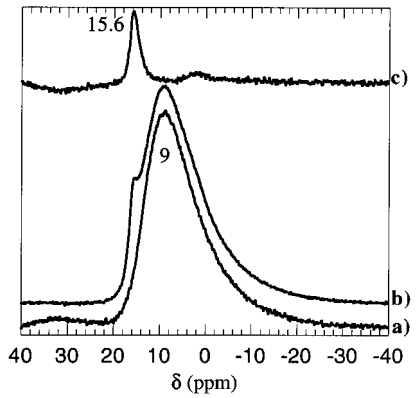

Figure 7. ^{27}Al CP-MAS NMR spectra of (a) Al_2O_3, (b) MoO_x/Al_2O_3 prepared at pH 4 (168 h), and (c) difference of (spectrum b−spectrum a).

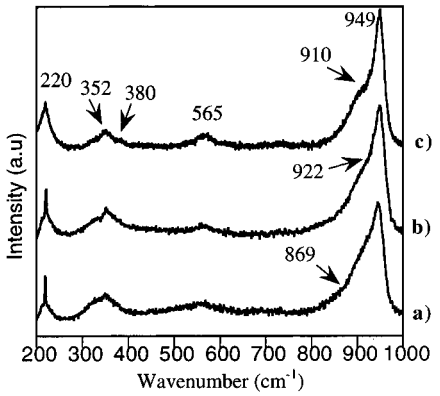

Figure 8. Raman spectra of MoO_x/Al_2O_3 prepared at (a) pH 5.1 (168 h), (b) pH 4 (168 h), and (c) pH 4 (672 h).

support. This was the motivation for using cross-polarization (CP) MAS NMR: only the aluminum atoms in dipolar contact with hydrogen will be observed, excluding most of the aluminum atoms from the bulk.[36] Especially, CP should be very effective for the central Al in [AlMo$_6$] because it is coordinated to six hydroxyls.

Part of the ^{27}Al CP-MAS NMR spectrum of the bare alumina support is shown in Figure 7 (spectrum a). It shows one broad band at 9 ppm which is assigned to the (surface) octahedral aluminums of the support with spinel-derived structure.[36] The CP-MAS NMR spectrum of the solid equilibrated at pH 4 for 7 days is shown in Figure 7, spectrum b. As compared to the bare alumina, it shows an extra shoulder around 15−16 ppm. Subtracting the bare alumina spectrum from the MoO_x/Al_2O_3 spectrum after normalization reveals that there is indeed a symmetric, narrow peak with its maximum at 15.6 ppm and a line width of 300 Hz. The peak position and width leave little doubt that a substantial amount of [AlMo$_6$] is deposited on the support, in a sample containing 5.2 wt % of Mo (cf., Table 3).

(iii) Raman Spectroscopy. Raman spectroscopy is one of the most widely used methods for discriminating molybdates and molybdenum oxide species on the surface of alumina (see, e.g., Wachs[37] for a review). Figure 8 shows the spectra of two solids equilibrated for 168 h, at pH 5.1 (spectrum a) and pH 4 (spectrum b), and one solid equilibrated for 672 h at pH 4 (spectrum c). The two spectra a and b are essentially identical. Their main features are one broad band at 949 cm^{-1} with two more or less pronounced shoulders around 869 and 922 cm^{-1} and two bands at 352 and 220 cm^{-1}. One can also notice a

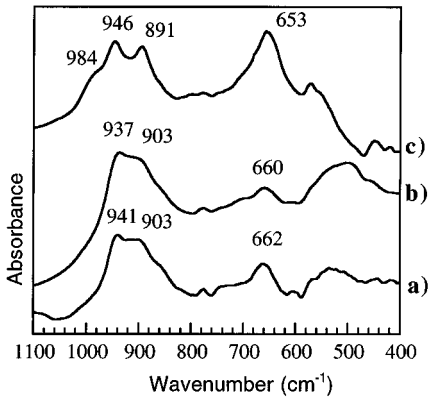

Figure 9. IR spectra of MoO_x/Al_2O_3 prepared at (a) pH 4 (168 h), (b) pH 5.1 (168 h), and (c) pH 4 (672 h). These spectra were obtained by subtracting the contribution of the alumina support.

weak band at 565 cm^{-1} (the sharp peak at 220 cm^{-1} is an experimental artefact due to a plasma line from the Ar^+ laser not removed by the interferential filter). Such spectra are characteristic for MoO_x/Al_2O_3 catalysts, and it can be safely concluded that the molybdenum species on the support are polymeric, since bands at 565 and 220 cm^{-1} are due respectively to Mo−O−Mo symetric stretches and deformations.[38]

However, it is not straightforward to discriminate [AlMo$_6$] from [Mo$_7$O$_{24}$]$^{6-}$ on the sole basis of these Raman spectra. Indeed, in the spectra of liquid-state reference compounds, the main difference between the Raman spectra of [AlMo$_6$] and [Mo$_7$O$_{24}$]$^{6-}$ lies in a peak located either at 910 or at 898 cm^{-1} (cf., Table 1; both species exhibit their most intense peak around 950 cm^{-1}). In view of the larger width of the bands observed for the solid state as compared to that in the liquid state, it is not surprising that the distinction between both polyanions may be blurred.

On the other hand, for the catalyst prepared at pH 4 for 672 h (spectrum c), Raman bands are better resolved due to the high Mo loading of this catalyst (8.8 wt %; cf., Table 3). This spectrum shows a high intensity band at 949 cm^{-1}, and we can now clearly distinguish one shoulder at 910 cm^{-1}, one band at 565 cm^{-1}, and two bands at 380 and 352 cm^{-1}. All of these bands are located at the same positions as the ones found for [AlMo$_6$] in liquid state (cf., spectrum a, Figure 2). It would appear then that the major species deposited on the support at this pH and equilibrium time is the Anderson-type heteropolyanion.

It has to be noted that Van Veen et al.[39] have previously reported a very similar spectrum for a 9.1 wt % Mo/Al_2O_3 catalyst. They attributed it to a surface precipitate without describing its structure. In view of our results, their spectrum was probably due to [AlMo$_6$] deposited on the support. However, precipitate formation was no doubt due to surface precipitation in their case, as evidenced by a large pH increase: as the pH was kept constant in the present study, the precise adsorption mechanism is likely to be different.

(iv) IR Spectroscopy. IR spectra of MoO_x/Al_2O_3 catalysts obtained at pH 4 (spectrum a) and pH 5.1 (spectrum b) after 168 h and at pH 4 after 672 h of equilibration (spectrum c) are shown in Figure 9. The contribution of the alumina support was subtracted in the 300−1000 cm^{-1} range.

The spectra of catalysts obtained after 168 h of equilibration at pH 4 and 5.1 (5.8 and 5.4 wt % Mo, respectively) exhibit

(36) Morris, H. D.; Ellis, P. D. *J. Am. Chem. Soc.* **1989**, *111*, 6045−6049.
(37) Wachs, J. E. *Catal. Today* **1996**, *27*, 437−455.
(38) Hu, H.; Wachs, I. E.; Bare, S. R. *J. Phys. Chem.* **1995**, *99*, 10897−10910.
(39) van Veen, J. A. R.; Witt, H. D.; Emeis, C. A.; Hendriks, P. A. J. M. *J. Catal.* **1987**, *107*, 579−582.

one broad band at 941−937 cm^{-1} with a shoulder at 903 cm^{-1} which can be attributed to Mo═O stretches and a weaker band at 662−660 cm^{-1} which can be attributed to Mo−O−Mo symmetric stretch. Due to the poor resolution of these subtractions, it seems questionable to identify other maxima as coming from molybdenum−oxygen vibrations.

If we consider the IR spectra of the model solid-state compounds $K_3[Al(OH)_6Mo_6O_{18}]$ and $(NH_4)_6[Mo_7O_{24}]$ shown in Figure 2, it appears that IR spectroscopy will not be able to discriminate these compounds on MoO_x/Al_2O_3 catalysts. Indeed, both catalysts exhibit one band at 660−662 cm^{-1} (648 cm^{-1} for the model compounds) and one band at 903 cm^{-1} (891−893 cm^{-1} for the model compounds). Only the band at 937−941 cm^{-1} ($\nu_{Mo=O}$) in the catalysts spectra could only be attributed to $[AlMo_6]$. Nevertheless, it seems unconvincing to draw any conclusion from the position of only one band: for instance, the Mo═O bond length in $Mo_7O_{24}^{6-}$ could be modified by its interaction with the support, resulting in a band shift.

On the other hand, for the catalyst containing 8.8% Mo (pH 4, 672 h, spectrum c) three bands are resolved at 891, 946, and 984 cm^{-1} that can clearly be attributed to the $[AlMo_6]$ Anderson species (cf., spectrum b, Figure 2 for the reference species).

As for Raman spectroscopy, we can conclude that the $[AlMo_6]$ species can be convincingly evidenced on the γ-alumina support by IR spectroscopy only for high Mo loading catalysts (8.8 wt %).

Discussion

Mo Speciation in Solution. All of the evidence on the liquid phase after equilibration (^{27}Al NMR, Raman, ^{95}Mo NMR) converges to show that the Anderson-type heteropolymolybdate, $[AlMo_6]$, is spontaneously formed in solution upon contact of γ-alumina with a solution of ammonium heptamolybdate in the pH range of 4−6.5. At higher pH values (pH 7 and 8), the only molybdate species in solution is MoO_4^{2-}. Our data on the kinetics of this phenomenon are limited so far, but we know that it is rather fast in the sense that it cannot be neglected on the time scale of the unit operations of catalyst preparation: the $[AlMo_6]$ polyanion is formed quantitatively after a few hours of equilibrium either at pH 4 or 6.1.

Raman spectroscopy shows that at pH 4, the $[AlMo_6]$ species is overwhelmingly predominent: no other Mo-containing species can be detected. This is in agreement with the systematic study of the aqueous $H^+-Al^{3+}-MoO_4^{2-}$ system performed by Öhmann.[18] The predominance diagram as calculated by this author shows that, in the presence of 10^{-3} M total Al in solution, $[AlMo_6]$ formation extends the domain of stability of the polymeric forms of molybdates into the basic region by at least one pH unit.

Evidence for the Formation of the $[AlMo_6]$ Heteropolyanion in the Adsorbed Phase: Relations with Earlier Studies. In the solid state, that is to say for MoO_x/Al_2O_3 catalysts, the two incontrovertible pieces of evidence for the presence of the Anderson-type anions on the surface after equilibration at pH 4 are ^{27}Al CP-MAS NMR, which is not a routine technique in most laboratories, and Raman−IR spectroscopies, but the latter only for a very high loading catalyst (8.8 wt %) obtained after 1 month of equilibration, which is not a typical equilibration time in catalyst preparation.

To summarize, discriminating isopolymolybdates (like heptamolybdate) from heteropolymolybdates (such as the $[AlMo_6]$ species) on alumina by the usual techniques used in catalyst characterization, such as UV−vis, IR, and Raman, is not straightforward due to the close structural relationship of the iso- and the heteropolymolybdate: both species are built from edge-sharing octahedra and will thus share many spectroscopic features.

These results may explain why thorough review articles on MoO_x/Al_2O_3 preparation[40] do not mention the possibility of the formation of $[AlMo_6]$.

Actually, starting in 1981, Goncharova et al.[22,24,41] tried to identify the $[AlMo_6]$ species deposited on γ-alumina from the IR spectra of MoO_x/Al_2O_3 catalysts in the Mo−O vibrations region, subtracting the bands of the support. Unfortunately in order to characterize $[AlMo_6]$ on the surface, they used the bands at 445 and 665 cm^{-1} and the presence of a triplet in the 880−950 cm^{-1} range as diagnostic. As already mentioned (see Figures 2 and 9 in particular), these criteria are not satisfactory to discriminate the heptamolybdate from the $[AlMo_6]$ species, especially in view of the poor resolution of spectra obtained by subtraction. This may be the reason why the work of Goncharova et al. has not gained more general recognition, although the basic chemical intuition was correct.

Nevertheless, it is interesting to note that ^{27}Al NMR peaks at approximately +15 ppm have occasionally been reported in the literature on alumina-supported Mo catalysts. Edwards and Decanio[42] have observed a peak at +13 ppm in the ^{27}Al CP-MAS spectrum of P-Mo/Al_2O_3 catalysts prepared by the incipient wetness method. They attributed it to a "hydrated form of an aluminum molybdate $Al_2(MoO_4)$" with tentative formula $[Al(OH)_n(H_2O)_{6-n}]_n(MoO_4)$, $n = 1$ or 2. This signal cannot be due to unhydrated $Al_2(MoO_4)$ which shows four peaks at negative δ values (between −10 and −15 ppm[43]). In light of our results, it is most likely that Edwards and Decanio have in fact observed the $[AlMo_6]$ polyanion.

It may be mentioned here that one team has used a Pt-containing heteropolymolybdate with an Anderson structure, $[PtMo_6O_{24}]^{8-}$, as a building block for "smart" bimetallic catalysts.[44] While its structure was maintained when it was deposited on silica, the polyanion broke down upon deposition on δ-alumina, as evidenced by the disappearance of EXAFS features associated with Pt−Mo neighbors. One may hypothesize that this is due to the high affinity of Al^{3+} for the Anderson-type structure. High-temperature reduction of the catalyst precursors obtained in this way resulted in metallic particles with very specific properties.

Relevance of the Formation of $[AlMo_6]$ for Supported Catalyst Preparation: (i) Deposition by Equilibrium Adsorption. Having established the reality of $[AlMo_6]$ formation in our systems, it is necessary to discuss how significant the phenomenon may be in realistic conditions for MoO_x/Al_2O_3 catalyst preparation. The currently used preparation method that is most related to our own is equilibrium adsorption, where a Mo-containing solution is left in contact with the alumina support until equilibria are completed, following which the excess liquid phase is removed and loosely held molybdenum is eventually washed away. In recent literature, the most carefully conducted study is due to Spanos et al.[45,46]

(40) Knözinger, H. In *Proceedings of the 9th International Congress on Catalysis*; The Chemical Institute of Canada: Ottawa, 1989 Calgary, 1988; pp 20−53.
(41) Goncharova, O. I.; Yur'eva, T. M.; Davydov, A. A. *Kinet. Catal.* **1986**, *27*, 816−822.
(42) Edwards, J. C.; Decanio, E. C. *Catal. Lett.* **1993**, *19*, 121−130.
(43) Haddix, G. W.; Narayana, M.; Tang, S. C.; Wu, Y. *J. Phys. Chem.* **1993,** *97*, 4624−4627.
(44) Liu, T.; Asakura, K.; Lee, U.; Matsui, Y.; Iwasawa, Y. *J. Catal.* **1992**, *135*, 367−385.
(45) Spanos, N.; Vordonis, L.; Kordulis, C.; Lycourghiotis, A. *J. Catal.* **1990**, *124*, 301−314.
(46) Spanos, N.; Vordonis, L.; Kordulis, C.; Koutsoukos, P. G.; Lycourghiotis, A. *J. Catal.* **1990**, *124*, 315−323.

Table 4. Comparison of Experimental Conditions between This Study and Studies of Spanos et al.[45,46]

	Spanos et al.	this study
initial [Mo] (mol L^{-1})	10^{-3} to 3×10^{-2}	6.4×10^{-2}
Al_2O_3 concentration $C_{Al_2O_3}$ (g L^{-1})	2.7	10
Al_2O_3 surface area S_S (m^2 g^{-1})	123	190
pH	4 to 10.5; drifts during equilibration	4 to 8; maintained constant
equilibration time	20 h	1 h to 7 days

Spanos et al. did not attempt to regulate pH during adsorption, and the reactions of the surface groups of alumina caused a drift to more basic pH during adsorption. This pH drift was important in the less-concentrated solutions, but remained <0.5 pH units provided $[Mo]_{initial}$ was $\geq 8 \times 10^{-3}$ M. Therefore, comparison with our results (Table 4) is appropriate and indicates that $[AlMo_6]$ was probably an important species in experiments performed on the acidic side, including at the natural pH of heptamolybdate solutions. Incidentally, the fact that $[AlMo_6]$ went unrecognized in this study probably does not affect the validity of its main conclusions: it is likely that $[AlMo_6]$, instead of heptamolybdate, is electrostatically adsorbed.

Relevance of the Formation of $[AlMo_6]$ for Supported Catalyst Preparation: (ii) Deposition by Incipient Wetness Impregnation—the "Buffer Effect" of Alumina. A majority of studies on MoO_x/Al_2O_3 use the so-called "incipient wetness impregnation" procedure. In this technique, there is no bulk liquid phase present; the heptamolybdate is dissolved into an amount of water barely sufficient to fill the porosity of the support. There is no washing of the solid material, but direct drying, forcing quantitative deposition of the molybdenum originally present in solution.

The question of the formation of $[AlMo_6]$ is then more difficult to solve. This is partly due to insufficient specification of the experimental parameters. For instance, the time of contact between the liquid phase in the porosity and the solid surface is often not specified, which forbids comparison with Al_2O_3 dissolution rates (although it may be argued that the ensuing drying step, at 90−120 °C, will speed up dissolution as long as some liquid phase remains).

The small amount of liquid phase with respect to solid support in the heterogeneous system is another, more fundamental, factor that complicates analysis. We have mentioned the ionization of alumina surface groups, a reaction that can be written, in the acidic pH range (pH < 8), as

$$Al{-}OH_2^+ \rightleftharpoons Al{-}OH + H^+ \qquad (9)$$

(conventionally written in this direction, but proceeding to the left here); the existence of this reaction implies that alumina can act as a pH buffer, provided that the number of ionizable Al−OH surface groups is at least comparable to the number of other species with acido−basic properties in the suspension (this fact is sometimes used for a crude determination of the point of zero charge of support materials[47,48]).

In the present case, molybdates are implied in two acido−basic reactions, namely, eqs 6 and 7. Therefore, the ionization of surface Al−OH can drive both eq 6 and 7 to the left, a fact that has often been recognized (a total of 1 proton per Mo is needed for eq 6 and of 8/7 protons per Mo for eq 9). The extent of this occurrence will depend on the ratio of ionizable surface Al−OH to total Mo in the suspension. The difficulty lies of course in estimating the first quantity: the concentration of ionizable surface Al−OH (in mole $gram^{-1}$) is the product of the surface area (S_s, in $meter^2$ $gram^{-1}$) and the surface density of ionizable Al−OH (Γ_{Al-OH}, in mole $meter^{-2}$ or equivalent units). Γ_{Al-OH} depends on factors such as the ionic strength of the solution, but values on the order of 0.3−2 nm^{-2} (i.e., 0.5−3.3 μmol m^{-2}) are typical.[45,46] Altogether, if $S_s\,\Gamma_{Al-OH} > [Mo]$ (molybdenum concentration in mole $gram^{-1}$), extensive depolymerization to monomolybdates will occur and $[AlMo_6]$ formation will not be the dominating feature of molybdate speciation. Taking a typical value of $S_s = 200$ m^2 g^{-1} for γ-Al_2O_3, one reaches the conclusion that all of the molybdenum could be converted to monomolybdate by the "buffer effect" of alumina up to $[Mo] = 6.6 \times 10^{-4}$ mol g^{-1} (which would correspond to a weight loading of 6 wt % Mo in the final catalyst).

The data of Luthra and Cheng[28] and of Sarrazin et al.[49,50] are particularly relevant for our discussion since they attempted to follow the speciation of molybdates in the porosity of alumina by liquid-state ^{95}Mo NMR during the course of the incipient wetness impregnation procedure.The only species detected in the solution were $Mo_7O_{24}^{6-}$ and MoO_4^{2-}, the latter indicating the occurrence of depolymerization reactions. Examination of the spectra does not reveal the signal characteristic of $[Mo_6Al]$, even when excess molybdate was present in the porosity (e.g., for $[Mo] = 1.6 \times 10^{-3}$ mol g^{-1} corresponding to 14 wt % Mo in Figure 1 of ref 50). However, quantification of total NMR-detectable Mo by Sarrazin et al. showed that up to 97% of the molybdenum introduced in the porosity became NMR-silent, which was rationalized as being due to restricted mobility of the adsorbed species. Therefore, these data are not incompatible with the presence of $[AlMo_6]$ among adsorbed species.

On the other hand, the already mentioned ^{27}Al CP-MAS NMR study of P-Mo/Al_2O_3 by Edwards and Decanio[42] also concerned catalysts prepared by incipient wetness impregnation; in that case, NMR observation carried out after calcination at 500 °C followed by exposure to air seems to reveal the existence of $[AlMo_6]$, raising the interesting possibility that even when this species is not formed directly from the deposition solution, it can still form later after thermal treatment followed by rehydration. The latter contention would of course need careful checking.

In any case, we may conclude that the formation of $[AlMo_6]$ can never be safely dismissed for MoO_x/Al_2O_3 catalysts prepared by the typical procedures referenced in the literature.

Rationalization of Supported Transition Metal Catalysts Preparation: the Support as a Reagent. We have shown in the present study that concepts derived from geochemistry can be of most importance in understanding the first stages of catalyst preparation, especially when we are considering the role of oxide supports. Indeed the support is usually considered as inert from a chemical point of view during the aqueous impregnation step in most studies on catalyst preparation. This idea is apparent, e.g., in the low reported solubility product of catalytic supports.[9] The contribution of geochemistry is to show that oxide dissolution is dependent on the nature of ligands in solution. This dependence can be either kinetic or thermodynamic as mentioned in the Introduction.

Our kinetic data are limited so far but from a thermodynamic point of view we have evidenced that the ability of molybdates

(47) Zalac, S.; Kallay, N. *J. Colloid Interface Sci.* **1992**, *149*, 233−240.
(48) Park, J. H.; Regalbuto, J. R. *J. Colloid Interface Sci.* **1995**, *175*, 239−252.
(49) Sarrazin, P.; Mouchel, B.; Kasztelan, S. *J. Phys. Chem.* **1989**, *93*, 904−908.
(50) Sarrazin, P.; Mouchel, B.; Kasztelan, S. *J. Phys. Chem.* **1991**, *95*, 7405−7408.

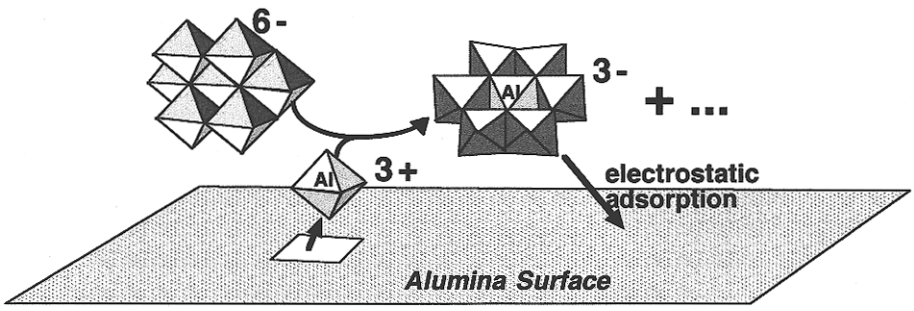

Figure 10. Schematic representation of the ligand-promoted alumina dissolution.

to complex aluminum ions greatly enhances alumina solubility. This is represented schematically in Figure 10 where isopolymolybdates act as inorganic ligands; one may notice the similarity to Figure 1 which depicts the type of process considered by geochemists when organic ligands are present in the solution.

Furthermore, the molybdic species that is deposited is not the heptamolybdate as commonly assumed, and this calls for a critical reevaluation of many published interpretations on the structure of supported molybdates.

We are currently considering the effect of thermal treatments on the structure of supported [$AlMo_6$]. This study will hopefully allow the assessment of the significance of the heteropolymolybdate for the control of the properties of the final catalyst.

Conclusion

When ammonium heptamolybdate was deposited on γ-Al_2O_3 by the equilibrium adsorption method, the Al-containing heteropolymolybdate $[Al(OH)_6Mo_6O_{18}]^{3-}$, or [$AlMo_6$], formed in the solution: in the pH range of 4−6, the Mo in the solution quantitatively transformed into [$AlMo_6$] within a few hours, as evidenced by various spectroscopic methods. Furthermore, the structure of [$AlMo_6$] was preserved in the adsorbed phase. The formation of this mixed species resulted in an increase of alumina solubility by several orders of magnitude.

The above results are the first clear example of an extensive metal−support chemical reaction in a case where the transition metal precursor is an *anionic* species. They indicate that oxide supports contacted with aqueous solutions, in addition to their other possible roles, may act as stoechiometric reagents, to provide a very strong metal−support interaction from the very first step of catalyst preparation. This fact, while long recognized by geochemists, has yet to be generally accepted in the community of heterogeneous catalysis, as witnessed by the near absence of references to [$AlMo_6$] formation in the extensive literature on MoO_x/Al_2O_3 systems.

Work is underway to study the thermal transformations of supported [$AlMo_6$] species and to generalize the concepts developped to related systems such as WO_x/Al_2O_3.

Acknowledgment. We are very grateful to Dr François Lucas for his help using the FullProf software, to Dr Jean-Baptiste d'Espinose de la Caillerie and Samuel Philippot for their help in performing solid state ^{27}Al measurements, and to Dr Geneviève Chottard for facilitating Raman measurements.

Supporting Information Available: Experimental details on the preparation and characterization of the reference heteropolymolybdate (XRD, UV) and quantification of ^{27}Al NMR (4 pages). See any current masthead page for ordering and Internet access instructions.

JA971981R